

Original Article

Cross-border regulation of the STK39/MAPK14 pathway by *Lycium barbarum* miR166a to inhibit triple-negative breast cancer

Yujin Hou^{1*}, Jing Li^{2*}, Xuan Li¹, Ye Lv¹, Chunxiu Yuan¹, Jia Tian^{3#}, Xinlan Liu^{4#}

¹Department of Oncology, General Hospital of Ningxia Medical University, Yinchuan, Ningxia, China; ²Department of Special Technical Diagnosis and Treatment, Ning'an Hospital, Yinchuan, Ningxia, China; ³Institute of Medical Sciences, General Hospital of Ningxia Medical University, Key Laboratory of Fertility Preservation and Maintenance of Ministry of Education, Ningxia Medical University, Yinchuan, Ningxia, China; ⁴Department of Medical Oncology, Ningxia Hui Autonomous Region Hospital, Yinchuan, Ningxia, China. *Equal contributors and co-first authors. #Equal contributors.

Received March 1, 2024; Accepted June 1, 2024; Epub June 15, 2024; Published June 30, 2024

Abstract: Objective: To investigate the effects of *Lycium barbarum* miRNA166a (Lb-miR166a) on human gene expression regulation during the therapy for triple-negative breast cancer (TNBC). Methods: Transcriptome sequencing was used to analyze the distribution and composition of miRNA in *Lycium barbarum* fruit. Lb-miR166a was introduced into TNBC MB-231 cells by lentiviral transfection to study its effects on cell proliferation, apoptosis, invasion, and metastasis both in vivo and in vitro. Bioinformatic and dual-luciferase assays identified the target gene of Lb-miR166a. The role of STK39 in TNBC progression was elucidated through clinical data analysis combined with cellular studies. The influence of Lb-miR166a on the STK39/MAPK14 pathway was confirmed using a target-specific knockout MB-231 cell line. Results: Lb-miR166a was found to be highly expressed in *Lycium barbarum*. It inhibited MB-231 cell proliferation, invasion, and metastasis, and promoted apoptosis. STK39 was overexpressed in TNBC and was associated with increased invasiveness and poorer patient prognosis. Gene enrichment analysis and dual-luciferase assays demonstrated that Lb-miR166a regulates STK39 expression cross-border and inhibits MAPK14 phosphorylation, impacting the phosphorylation of downstream target genes. Conclusion: The downregulation of STK39 and subsequent inhibition of MAPK14 phosphorylation by Lb-miR166a leads to reduced proliferation, migration, and invasion of TNBC cells. These findings suggest a novel therapeutic strategy for TNBC treatment, highlighting possible clinical applications of Lb-miR166a in managing this aggressive cancer type.

Keywords: *Lycium barbarum*, miRNA, triple negative breast cancer, STK39, MAPK14, MAPK signaling pathway

Introduction

Despite advances in research and clinical treatment, breast cancer continues to be a leading cause of cancer-related deaths among women [1]. According to the GLOBOCAN 2020 report, breast cancer has now become the most commonly diagnosed cancer in women, representing 30% of all female cancers, with a persistently high mortality rate [2]. Over the past 25 years, there has been a continuous increase in both the incidence and mortality rates of breast cancer globally [3], especially for triple-negative breast cancer (TNBC). TNBC is known for its poor differentiation, high invasion rate, frequent recurrence, metastasis, and substantial

drug resistance [4]. Patients with TNBC have a 40% mortality rate within five years of diagnosis and an average recurrence time of 19-40 months; those with recurrence within three months face a 75% mortality rate [5]. Consequently, developing more effective drugs to enhance the survival rate or provide precise treatment for TNBC is an urgent priority and the focus of ongoing research.

Recent evidence over the past decade indicates that plant-derived miRNAs can regulate gene expression in animals, affecting physiologic processes and disease progression [6]. These findings have spurred interest in extracting specific substances from plants for use as

additives and in exploring the mechanisms of Chinese herbal medicines in disease treatment, broadening the research scope for exogenous animal and plant miRNAs. Thus, in-depth study of the mechanisms and roles of plant-derived miRNAs through cross-species regulation is essential for human health and development [7].

Lycium barbarum L., a traditional Chinese medicine and a valuable food resource, exhibits various biological activities including anti-aging, anti-oxidation, metabolic enhancement, immune regulation, and anticancer effects [8-10]. However, the exact role and mechanism of *Lycium barbarum* miRNA in regulating human gene expression for the treatment of triple-negative breast cancer remain largely unexplored, necessitating further research. This study highlights how Lb-miR166a targets the STK39/MAPK14 pathway to inhibit the progression of TNBC.

Materials and methods

Tissue samples and cell line culture

Tissue samples from 48 surgical resections, paired with adjacent non-carcinoma tissues from patients with primary TNBC, were collected at the General Hospital of Ningxia Medical University between January 2023 and December 2023 to analyze STK39 expression. None of the patients had received chemoradiotherapy or biological treatment prior to surgery, and the specimens were preserved at -196°C in liquid nitrogen. Additionally, to assess the impact of STK39 expression on long-term prognosis, 109 patients with available STK39 expression and survival data from January 2018 to January 2019 were included. This study received approval from the Institutional Medical Ethics Committee of the General Hospital of Ningxia Medical University, and all patients provided informed consent for the use of their tissue specimens. MB-231 human TNBC cells were obtained from the National Biomedical Cell-Line Resource (Beijing, China) and cultured in RPMI-1640 medium (Gibco) supplemented with 10% fetal bovine serum (FBS) (Gibco) and 1% penicillin-streptomycin (Sigma-Aldrich, Merck, Germany), at 37°C and 5% CO_2 .

*Sequence analysis of *Lycium barbarum* miRNA*

miRNA sequencing of *Lycium barbarum* was conducted by Genecreate Company (Wuhan, Hubei, China). Total RNA was extracted using TRIzol reagent, and RNA integrity was assessed using a NanoDrop (Thermo Scientific, US). Sequencing was carried out on the Illumina HiSeq2500 platform. Image analysis of the acquired arrays was performed using Agilent Feature Extraction software (version 11.0.1.1). Data processing, including quantile normalization, was conducted using the R software package *limma*. Volcano plot filtering was applied to identify significantly differentially expressed miRNAs between the two groups. Differential expression analysis was conducted based on normalized deep sequencing counts in RPM (Reads Per Million) using DESeq2. miRNAs with \log_2 fold changes ($\text{Log}_2\text{FC} \geq 1$) were classified as up-regulated, and those with negative values ($\text{Log}_2\text{FC} \leq -1$) as down-regulated. Hierarchical clustering was performed to visualize distinct miRNA expression patterns among the samples.

Construction of STK39 target-specific knockout cell line

The target sequence of Lb-miR166a is located in the 3'-untranslated region (3'UTR) of the STK39 gene. The STK39 target-specific knockout cell line was developed by OBiO Technology (Shanghai, China), using the CRISPR/Cas9 gene editing technique to delete the DNA sequence within the STK39 gene that interacts with Lb-miR166a. Electrotransfer was employed to knock out the target genes in the cells, followed by the isolation and culturing of single cells for monoclonal expansion. PCR and sequencing confirmed the acquisition of positive monoclonal cells lacking the target gene sequence.

Cell experiment groups

The MB-231 cells were categorized into several groups based on the effects of lentivirus transfection: ① N-group: Normally cultured MB-231 cells. ② Lb-miR166a group: Cells transfected with Lb-miR166a mimic lentivirus (MOI, 1:20). ③ L-group: Cells transfected with a control lentivirus (MOI, 1:20). ④ STK39cKo group: MB-231 cells with the target binding sequence of

STK39/MAPK14 in triple-negative breast cancer

Table 1. Primer sequences

Gene	Forward Primer	Reverse Primer
Lb-miR166a	ACACTCCAGCTGGGTCGGACCAGGCTTCA	TGGTGTCTGGAGTCG
STK39	TCTGCTGGCTTGGTGGATG	AGGGAGGGTTGAAGGGAGTAG
β -actin	CATGTACGTTGCTATCCAGGC	CTCCTTAATGTCACGCACGAT
U6	CTCGCTTCGGCAGCACA	AACGCTTCACGAATTTGCGT

the STK39 gene knocked out. ⑤ STK39sh group: MB-231 cells transfected with an STK39 interfering lentivirus.

The Lb-miR166a mimic and the STK39 interfering lentivirus were supplied by OBiO (Shanghai, China). The sequence of the Lb-miR166a miRNA mimic was 5'-TCGGACC-AGGCTTCATTCCCC-3'.

MB-231 cell mRNA sequence analysis

mRNA sequencing was conducted at Gene-Create (Wuhan, China). RNA was extracted using the TRIZOL method, and transcriptional sequencing was performed using the NovaSeq 6000 system (Illumina). Sequencing data were aligned using the Hisat2 software.

Dual-luciferase reporter assay

To determine whether Lb-miR-166a directly targets STK39, luciferase reporter assays were performed. Wild-type (WT) and mutant-type (MUT) 3'-UTRs of STK39 were transfected into 293T cells along with synthetic Lb-miR-166a mimic or negative control (NC) mimic. Post-transfection, cells were lysed, and the activities of Renilla and Firefly luciferases were measured using a dual-luciferase reporter system (Promega, USA) according to the manufacturer's instructions. Results were expressed as the ratio of Renilla luciferase (experimental) to Firefly luciferase (control).

Real-time quantitative polymerase chain reaction (qRT-PCR)

Total RNA was extracted from tumor cells using TRIzol reagent (Invitrogen) and quantified using a NanoDrop spectrophotometer (NanoDrop Technologies). cDNA was synthesized using Hifair® III 1st Strand cDNA Synthesis SuperMix (Yeasen, Shanghai, China). qRT-PCR was then performed on an ABI 7900 system (Thermo Fisher Scientific) using SYBR Green Real-Time PCR Master Mixes (Thermo Fisher

Scientific). Gene expression levels were normalized to β -actin and U6, and relative expression levels were calculated using the $2^{-\Delta\Delta Ct}$ method. Specific primer sequences are listed in **Table 1**.

Cell cycle analysis using flow cytometry

Cell cycle progression was analyzed using cell cycle test kits from KeyGEN Biotech (Jiangsu, China, KGA512). Cells were trypsinized (0.25% trypsin), collected, washed, and fixed in 70% cold ethanol at 4°C overnight before being centrifuged. Subsequently, 500 μ L of prepared propidium iodide (PI) staining solution was added to each sample. The samples were then incubated in the dark at 37°C for 30 minutes, followed by cell cycle analysis using flow cytometry.

Cell apoptosis detection using flow cytometry

The apoptosis rate was determined using apoptosis test kits from KeyGEN Biotech (Jiangsu, China, KGA1017). Cells were resuspended in PBS, washed, and then incubated with an Annexin V-PE mixture in the dark for 15 minutes. Afterwards, 7-AAD (7-amino actinomycin D) was added, and the mixture was further incubated for 5 minutes. Apoptosis ratios were then measured using flow cytometry.

Cell invasion assay

The cells from each group were collected and the cell concentration was adjusted to 2×10^5 /mL. The cell suspension was mixed with 10% fetal bovine serum and added to the upper chamber of a Transwell apparatus coated with Matrigel (BD Biosciences). Cells were cultured for 48 hours in DMEM culture medium in the lower chamber. After incubation, cells in the upper chamber were removed, and those that had invaded through the Matrigel were stained with crystal violet. The number of invaded cells was counted in three random fields under a microscope.

STK39/MAPK14 in triple-negative breast cancer

Wound healing assay

Cells (1×10^5) were seeded in 6-well plates and allowed to adhere overnight. A wound was created using the tip of a 10- μ L pipette, and images were captured at 0, 24, 48, and 72 hours using a light microscope (Zeiss, Shanghai, China). Wound closure was monitored and measured at each time point to assess cell migration.

Western blot detection

Following digestion with 0.25% trypsin, cells from each group were collected and lysed for protein extraction. Proteins were separated using 8%-15% SDS-PAGE gels. Primary antibodies were incubated overnight at 4°C, while secondary antibodies were incubated at 37°C for 1 hour. Protein bands were detected using ECL chemiluminescence and quantified with ImageJ 1.46R software. Antibodies were sourced from Proteintech Group (Wuhan, China) and Boster Biological Technology (Wuhan, China). Specific antibodies and their dilutions included: CCND1 (60186-1-Ig, 1:20000), PCNA (60097-1-Ig, 1:10000), CCNE2 (11935-1-AP, 1:10000), CCNA2 (66391-1-Ig, 1:10000), Vimentin (60330-1-Ig, 1:3000), E-cadherin (60335-1-Ig, 1:5000), N-cadherin (66219-1-Ig, 1:5000), Snail (13099-1-AP, 1:1000), Caspase3 (66470-2-Ig, 1:3000), BCL2 (68103-1-Ig, 1:10000), BAX (60267-1-Ig, 1:10000), MAPK14 (14064-1-AP, 1:2000), p-MAPK14 (28796-1-AP, 1:2000), and STK39 (M02516-2, 1:1000). Additional antibodies from Invitrogen (California, US) included MK2 (PA5-109937, 1:1000), Phospho-MK2 (PA5-12619, 1:1000), GSK3B (PA5-29251, 1:3000), Phospho-GSK3B (44-604G, 1:1500), SMAD3 (51-1500, 1:1000), Phospho-SMAD3 (44-246G, 1:1000), ATF2 (PA5-86110, 1:500), and Phospho-ATF2 (PA1-4613, 1:1000).

Establishment and grouping of animal models

All procedures involving animals were approved by the Institutional Animal Care and Use Committee of General Hospital of Ningxia Medical University, China. Eight-week-old female nude mice were sourced from Spiff Biotechnology Co., LTD (Beijing, China). Breast cancer cells (2×10^6) from each experimental group (N-group, Lb-miR166a group, and STK39cKo group) were subcutaneously inoculated on both sides of the abdomen, with three

mice per group, to establish a model of human breast cancer tumor transplantation. After 21 days, mice were euthanized using an overdose of anesthetic (pentobarbital sodium > 150 mg/kg), and subcutaneous tumor tissues were collected for analysis. Tumor volumes were calculated using the formula: volume (mm^3) = (width² × length)/2.

Detection of tumor liver metastasis

The breast cancer cells (2×10^6) from the N-group or the Lb-miR166a group were administered intravenously by tail vein injections into nude mice. After 21 days, the mice were euthanized with an overdose of anesthetic, and the livers were examined for tumor metastases.

Statistical analysis

Statistical analysis was performed using SPSS version 24.0, and data visualization was performed with GraphPad Prism version 7.0. Results were expressed as means ± standard deviations ($\bar{x} \pm \text{sd}$). Differences between two groups were assessed using an independent sample t-test, while one-way analysis of variance (ANOVA) was used to compare means across multiple groups. Dunnett's test was applied for post-hoc comparisons between two groups. A *p*-value of less than 0.05 was considered significant.

Results

Cross-regulation of multiple genes and signaling pathways by Lb-miR166a in MB-231 cells

Transcriptome sequencing identified 32 miRNAs (miRNAs) in *Lycium barbarum* (**Figure 1A**), with their sequences provided in [Supplementary Table 1](#). Among these, Lb-miR166a was highly expressed in the fruit of *Lycium barbarum*. Database searches revealed 7,361 potential target genes (score > 50) for the 32 miRNAs, including 3,139 with a higher confidence score (> 70) (**Figure 1B**).

In an experimental setup, two groups of mice ($n=6$ per group) were studied: one received a daily intragastric dose of 3 g of *Lycium barbarum* solution, while the control group was maintained on a standard diet. After one week, serum levels of Lb-miR166a were detectable in the *Lycium barbarum* group but not in the control group (**Figure 1C**).

STK39/MAPK14 in triple-negative breast cancer

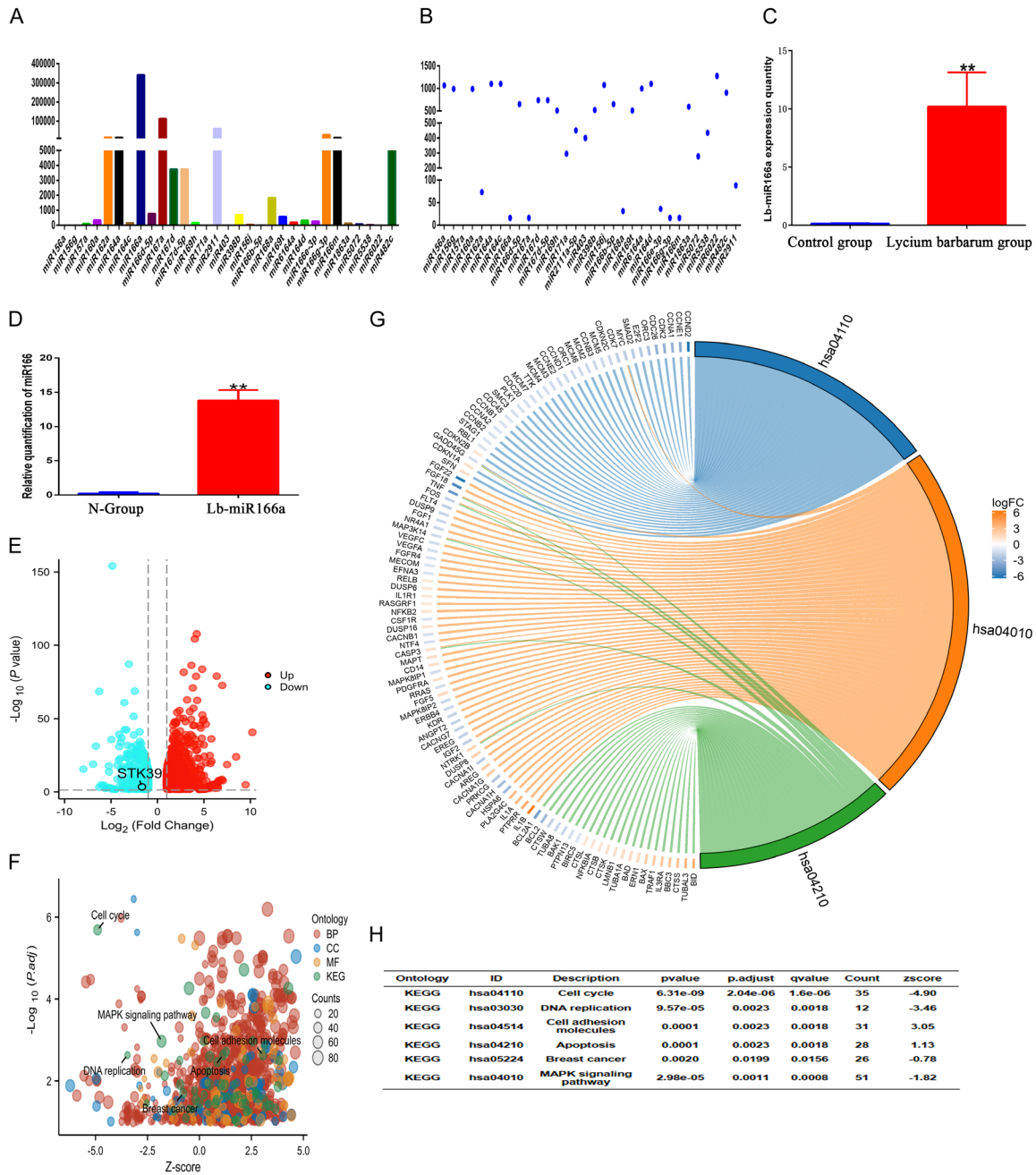


Figure 1. Regulation of gene expression and signaling pathways by Lb-miR166a in breast cancer cells. A. Sequencing and relative quantitative analysis of miRNA from Lycium barbarum L. B. Number of predicted target genes in humans regulated by Lycium barbarum miRNA. C. Levels of Lb-miR166a detected in mouse blood. D. Expression of Lb-miR166a assessed by quantitative PCR. E. Transcriptome sequencing for gene expression analysis. F. Functional cluster analysis of differentially expressed genes. G, H. Regulation of multiple KEGG signaling pathways by Lb-miR166a in breast cancer cells, including the cell cycle, MAPK, apoptosis, and DNA replication pathways. Red indicates up-regulation; green indicates down-regulation. ** $P < 0.01$. Control group: normal control mice. Lycium barbarum group: mice fed a diet supplemented with Lycium barbarum.

Lb-miR166a was introduced into MB-231 breast cancer cells using lentiviral transfection. Quantitative PCR (Q-PCR) analysis showed a significant increase in Lb-miR166a levels in the

treated group compared to the controls (**Figure 1D**; $P < 0.01$). mRNA sequencing indicated that Lb-miR166a influenced the expression of numerous genes, with 1,356 genes upregulat-

ed and 723 downregulated in the treated cells compared to controls (**Figure 1E**).

Functional analysis of these differentially expressed genes revealed that Lb-miR166a modulated several key signaling pathways related to breast cancer, including the cell cycle, MAPK, apoptosis, and DNA replication pathways (**Figure 1F-H**; $P < 0.01$).

Effects of Lb-miR166a on MB-231 cells in vivo and in vitro

Cell cycle analysis revealed an increase in the proportion of cells in the G1 phase and a decrease in the G2 and S phases within the Lb-miR166a group compared to the N group, which was statistically significant ($P < 0.01$). This suggests that Lb-miR166a impedes the progression of breast cancer cells from G1 to S phase (**Figure 2A, 2B**).

Western blot analysis indicated a downregulation of cell cycle-related proteins CCNA2, CCNE2, and CCND2 in the Lb-miR166a group compared to the N group, suggesting an inhibition of breast cancer cell proliferation by Lb-miR166a (**Figure 2C, 2D**; $P < 0.01$).

Apoptosis rates significantly increased in the Lb-miR166a group, as confirmed by flow cytometry results (**Figure 2E, 2F**; $P < 0.01$). Concurrently, western blot results showed increased expression of the pro-apoptotic proteins Caspase3 and Bax and decreased expression of the anti-apoptotic protein Bcl2 in the Lb-miR166a group compared to the N group (**Figure 2G, 2H**; $P < 0.01$).

In the wound healing assay, there was a significant increase in the residual area of the cell scratch in the Lb-miR166a group compared to the N group, indicating inhibited migration (**Figure 2I, 2J**; $P < 0.01$). Furthermore, Transwell migration assays showed a marked reduction in the invasion capability of the Lb-miR166a group cells compared to the N group (**Figure 2K, 2L**; $P < 0.01$).

Western blot analysis also revealed significant reductions in the expression of epithelial-mesenchymal transition (EMT)-related proteins Snail and N-cadherin, with a concomitant increase in E-cadherin levels in the Lb-miR166a group (**Figure 2M, 2N**; $P < 0.01$).

In vivo experiments in nude mice showed that the Lb-miR166a group exhibited significantly reduced subcutaneous tumor volumes and fewer liver metastases compared to the N group (**Figure 2O-S**; $P < 0.01$).

Lb-miR166a cross-border targeted regulation of STK39 protein expression

Bioinformatic analysis identified a targeted regulatory site between Lb-miR166a and human STK39 mRNA. This interaction was further validated by a dual-luciferase assay confirming the regulatory relationship (**Figure 3A, 3B**).

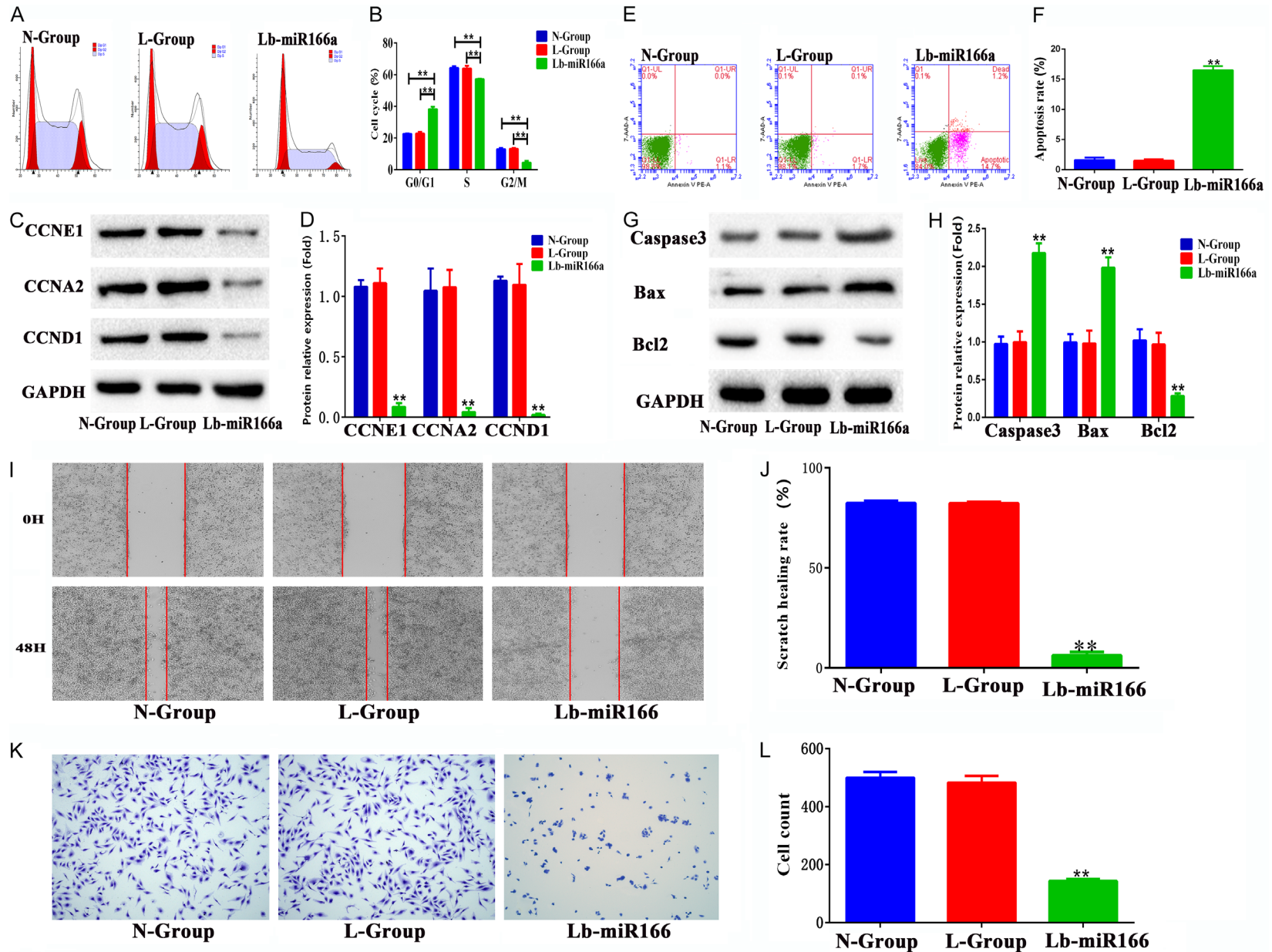
Role of STK39 expression in breast cancer progression and prognosis

STK39 plays a crucial role in influencing the biological behavior of MB-231 cells. High expression of STK39 in TNBC tissues was associated with poor prognosis (**Figure 4A, 4B**; $P < 0.01$). Downregulation of STK39 by lentiviral transfection in MB-231 cells significantly inhibited cell proliferation (**Figure 4C-F**; $P < 0.01$), promoted apoptosis (**Figure 4G-J**; $P < 0.01$), and suppressed invasion and metastasis, along with the downregulation of EMT-related genes (**Figure 4K-P**; $P < 0.01$). In vivo experiments in nude mice confirmed that inhibiting STK39 expression significantly reduced tumor proliferation and liver metastasis (**Figure 4Q-U**; $P < 0.01$).

Lb-miR166a regulation of the STK39/MAPK14 pathway

Further investigations confirmed that Lb-miR166a targets the 3'UTR region of the STK39/MAPK14 pathway. Knocking out the STK39 target sequence in MB-231 cells did not affect the expression of STK39 mRNA and protein (**Figure 5A-F**; $P > 0.05$). Immunofluorescence and western blot analyses showed that Lb-miR166a downregulated the expression of STK39 protein and that of p-MAPK14, inhibiting its nuclear translocation (**Figure 5G-J**; $P < 0.05$). However, these effects of Lb-miR166a were nullified when the binding target sequence was knocked out (**Figure 5N-Q**; $P > 0.05$). Additionally, western blotting revealed that Lb-miR166a reduced the phosphorylation of downstream MAPK14 targets, including MK2, GSK3 β , SMAD3, and ATF2,

STK39/MAPK14 in triple-negative breast cancer



STK39/MAPK14 in triple-negative breast cancer

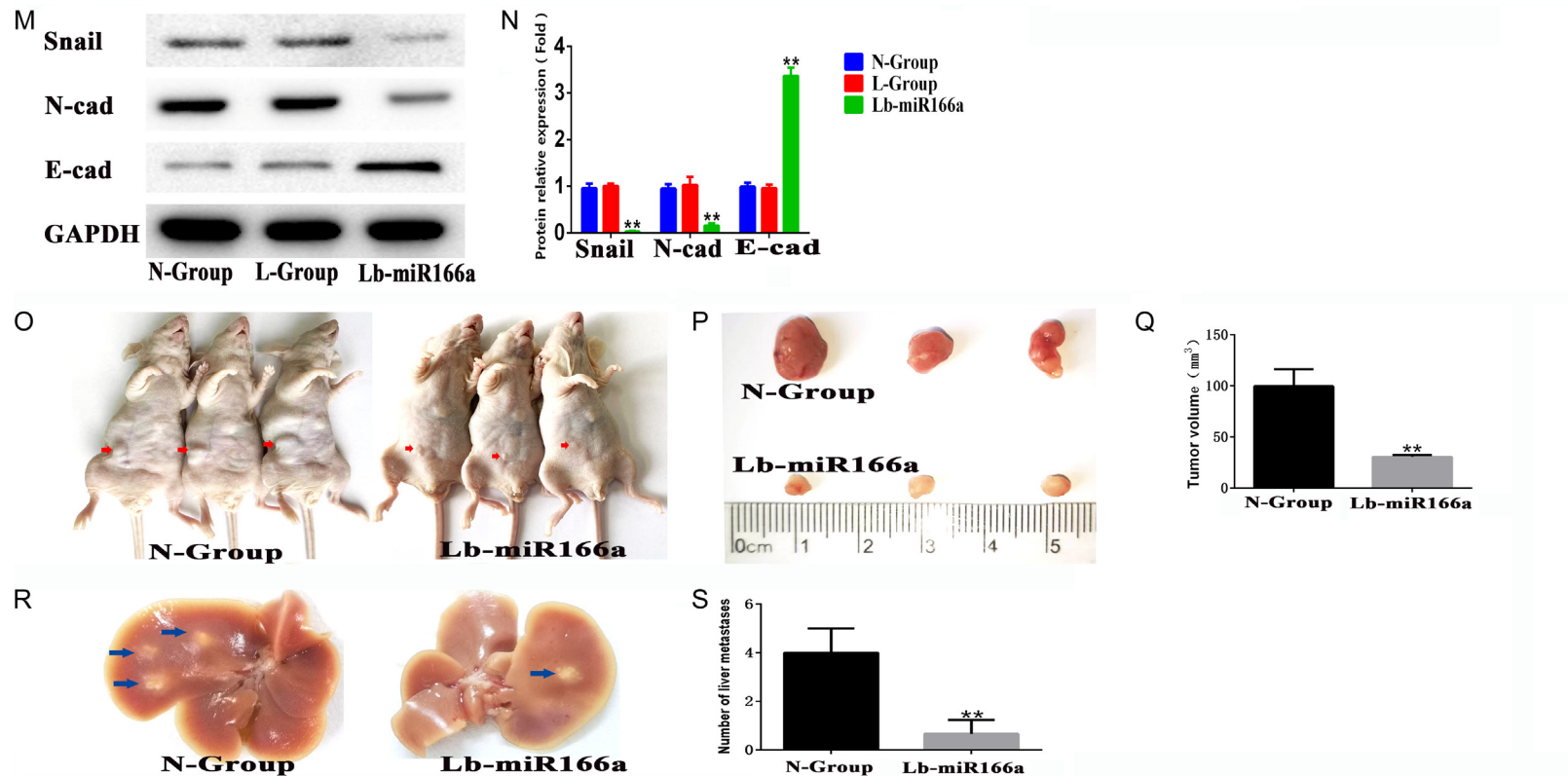


Figure 2. Lb-miR166a inhibits cell cycle progression, invasion, and migration, and promotes apoptosis in breast cancer MB-231 cells. A-D: Lb-miR166a suppresses MB-231 cell proliferation by regulating cell cycle progression. E-H: Lb-miR166a induces apoptosis in MB-231 cells. I, J: Lb-miR166a reduces migration of breast cancer MB-231 cells. K, L: The effect of Lb-miR166a on MB-231 cell invasion was assessed using a Transwell invasion assay. M, N: Effects of Lb-miR166a on the expression of EMT-related genes, as determined by western blot analysis. O-Q: The influence of Lb-miR166a on tumor proliferation was evaluated through a subcutaneous tumor xenograft experiment in nude mice. R, S: The effect of Lb-miR166a on tumor metastasis was examined by analyzing liver metastasis in nude mice. **P < 0.01. N-Group: Normal control group; L-group: Lentiviral control group; Lb-miR166a: Lb-miR166a overexpression group.

STK39/MAPK14 in triple-negative breast cancer

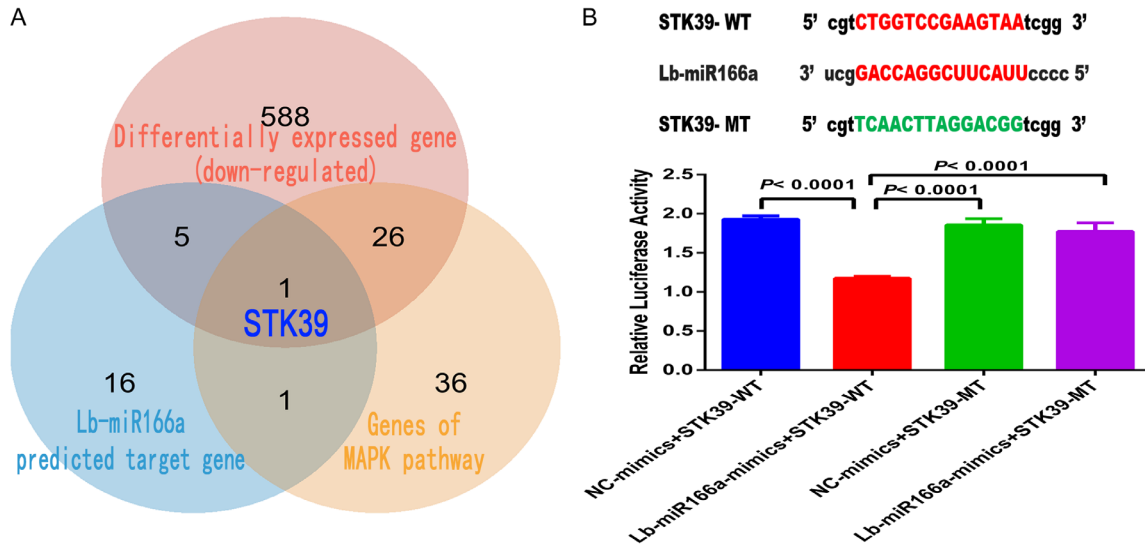


Figure 3. Targeted regulation of STK39 gene expression by Lb-miR166a. A. Transcriptome sequencing combined with bioinformatic analysis identified STK39 as a direct target of Lb-miR166a in the regulation of the MAPK signaling pathway. B. A dual-luciferase assay demonstrated the specific targeting of the STK39 gene by Lb-miR166a, confirming its role in modulating gene expression within this pathway.

highlighting its regulatory influence on the STK39/MAPK14 pathway (**Figure 5K-M**; $P < 0.05$). Yet, these regulatory effects were notably diminished in STK39cKo MB-231 cells (**Figure 5R-T**; $P > 0.05$).

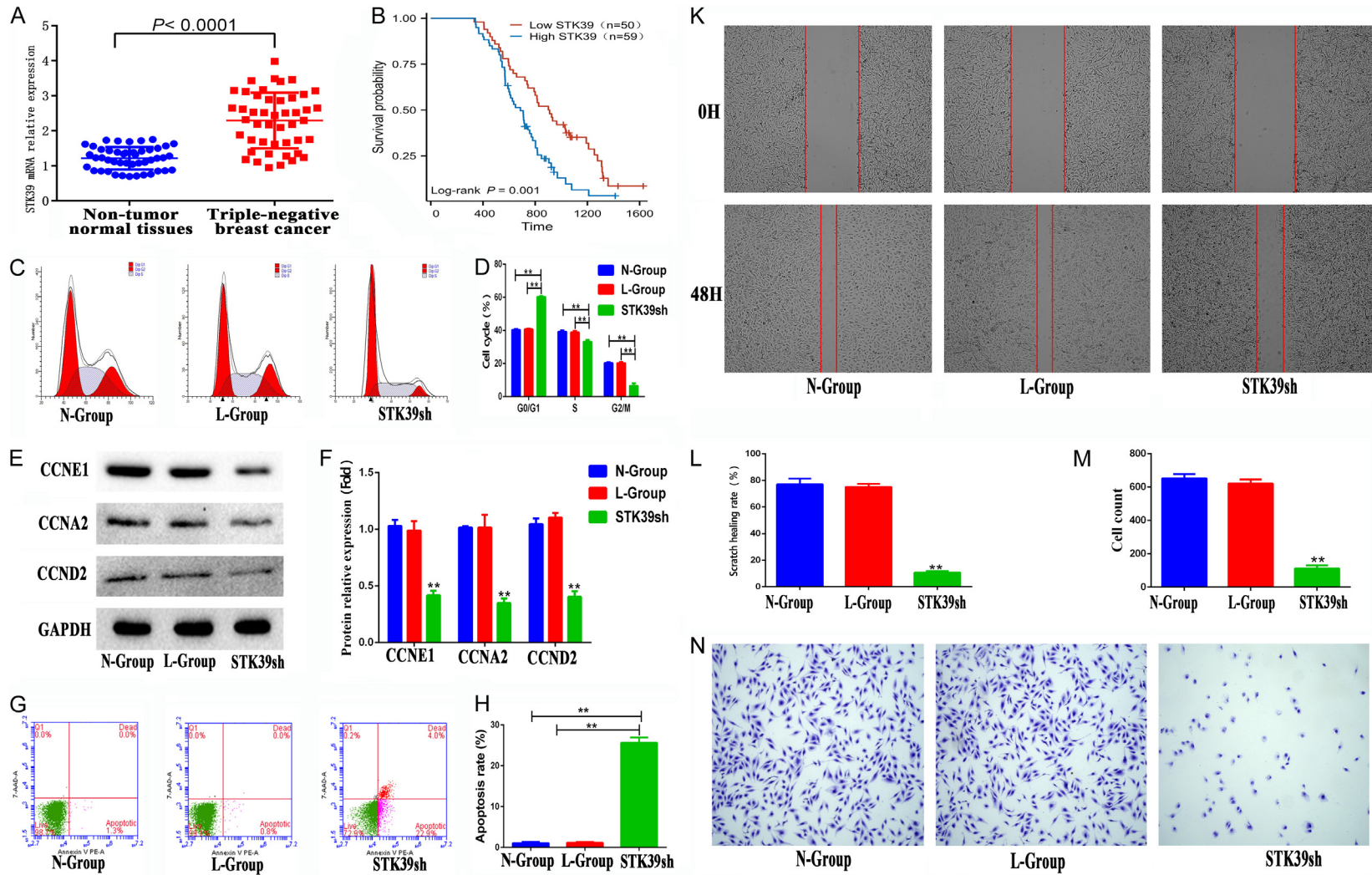
Discussion

Recurrence and metastasis of breast cancer are typically associated with poor prognosis and increased disease-related mortality [11]. Metastatic breast cancer represents 6%-10% of new cases, and it is estimated that 20-30% of all breast cancers will metastasize [12]. Therefore, discovering more effective drugs for precise treatment and improved survival is a crucial focus of current research. Phytochemicals have long been a primary source of bioactive substances with anticancer properties, playing key roles in modulating signaling pathways involved in cancer pathogenesis and progression. The screening and exploration of new plant-derived compounds is vital for development of anticancer drugs that are both low in toxicity and high in efficiency. Recent research has highlighted that plant-derived miRNAs in food, as single-stranded non-coding miRNAs, are functional food components that regulate physiological processes in animals [13].

In our study, we identified 32 miRNAs in the fruit of *Lycium barbarum*, with Lb-miR166a being the most abundant. Transfection of Lb-miR166a into breast cancer MB-231 cells led to a significant inhibition of cell proliferation and promotion of apoptosis. Transcriptome sequencing analysis showed a marked down-regulation of the MAPK signaling pathway, suggesting an anti-tumor role for Lb-miR166a through this pathway. This miRNA targeting mRNA mechanism is consistent with findings from other studies. For instance, Zhang et al. [14] reported that Lb-miR166a regulated the expression of various genes and affected numerous signaling pathways related to tumor development in kidney cancer. Our findings indicate that Lb-miR166a regulates the MAPK signaling pathway and downstream gene functions by targeting STK39/MAPK14, elucidating a possible mechanism for its anti-tumor effects in breast cancer.

We have discovered that STK39 is highly expressed in breast cancer, and its overexpression is associated with poor prognosis, a pattern also observed in other cancer types of cancer such as non-small cell lung cancer and osteosarcoma [15, 16]. Furthermore, STK39 is implicated in regulating tumor cell proliferation, migration, and invasion across various cancers, including osteosarcoma and cervical can-

STK39/MAPK14 in triple-negative breast cancer



STK39/MAPK14 in triple-negative breast cancer

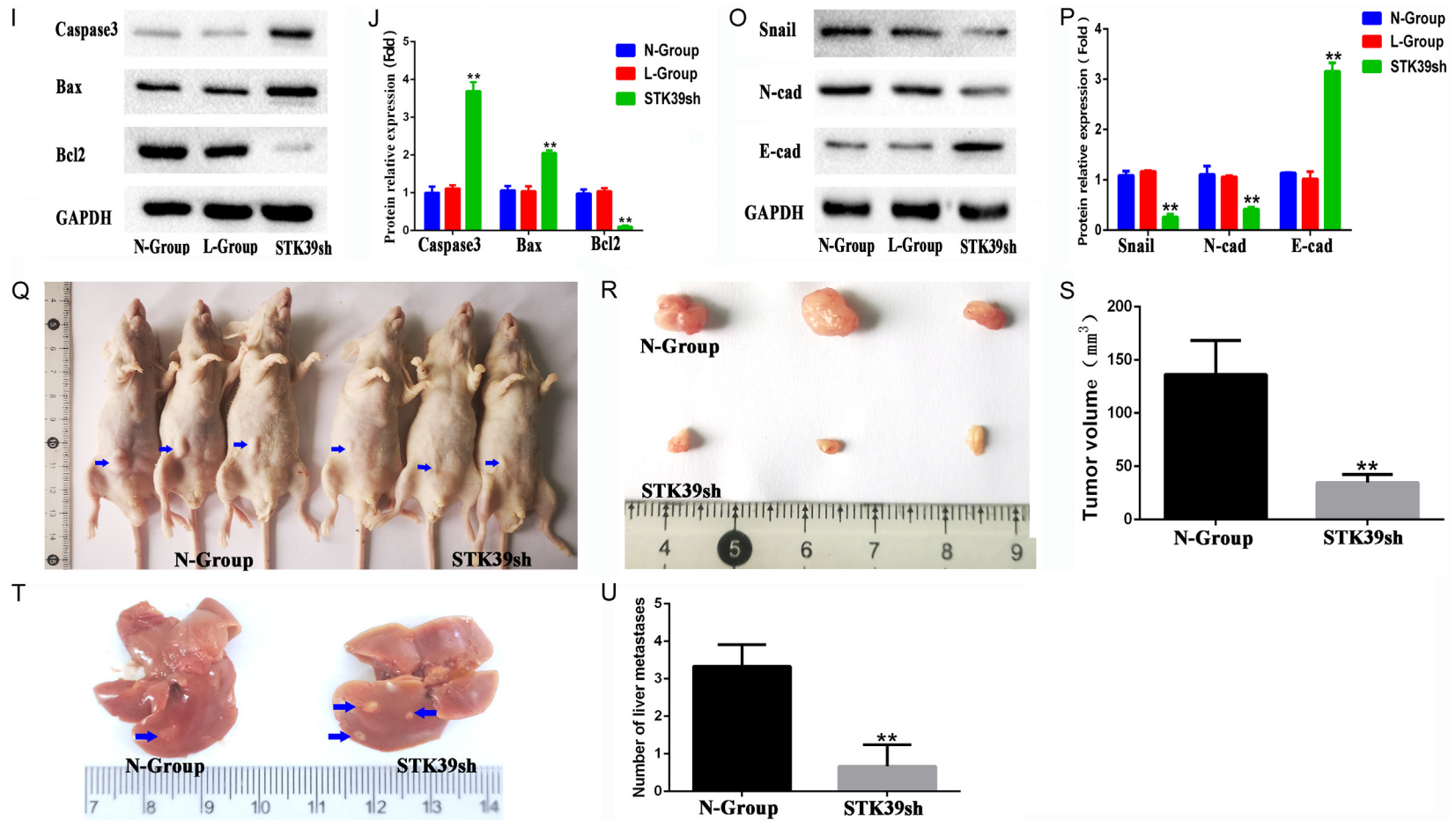
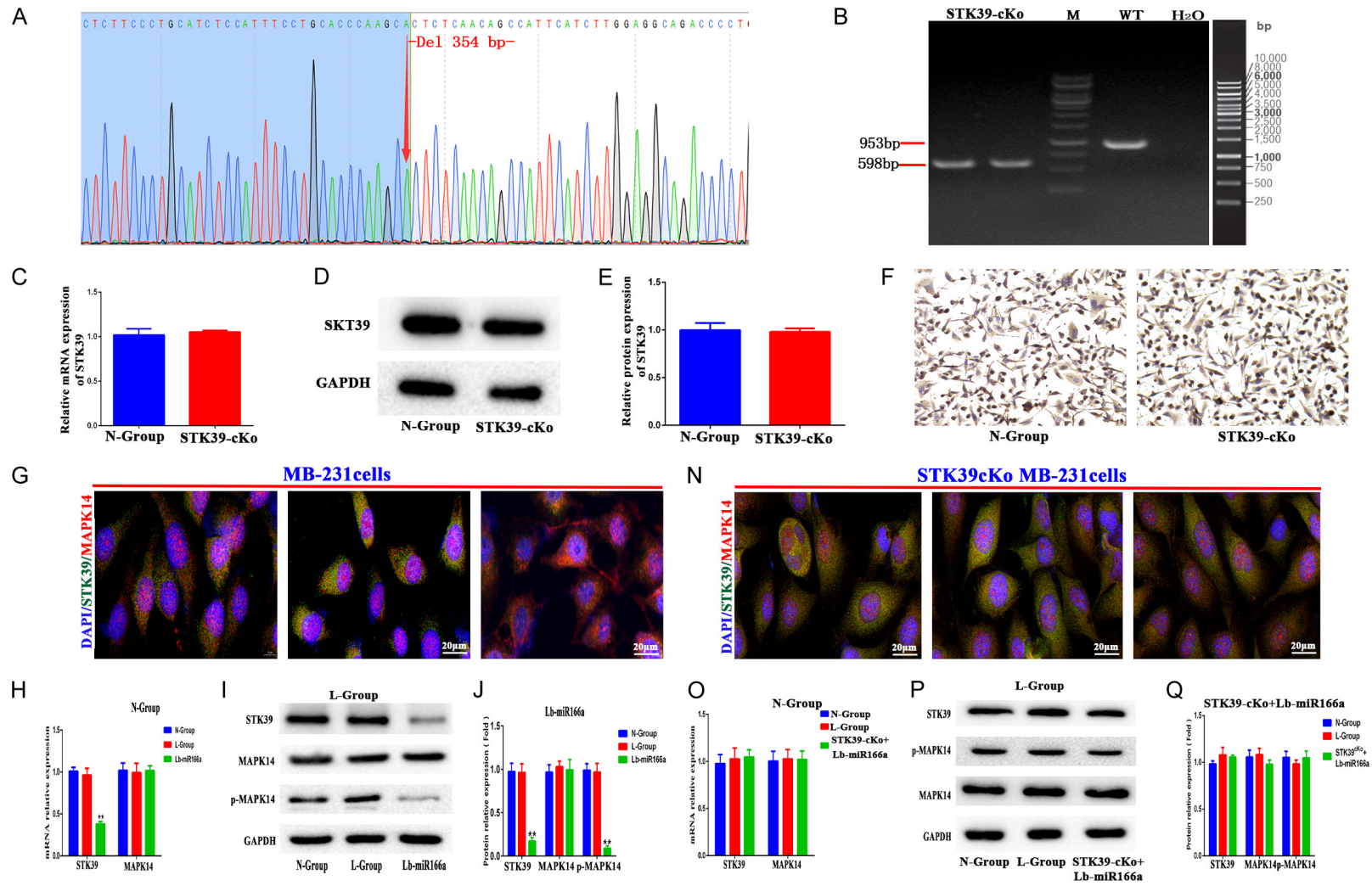


Figure 4. Role of STK39. A. High expression of STK39 observed in breast cancer tissue. B. Overexpression of STK39 is linked to poor prognosis. C, D. The impact of STK39 on the cell cycle was analyzed using flow cytometry. E, F. Expression levels of genes related to cell cycle regulation were assessed by western blot. G, H. The influence of STK39 on apoptosis was evaluated using flow cytometry. I, J. Western blot was used to detect the expression of genes regulating apoptosis. G-K. Down-regulation of STK39 leads to reduced invasion, migration, and epithelial-mesenchymal transition (EMT) in breast cancer MB-231 cells. K, L. The effect of STK39 on cell migration was assessed through a scratch assay. M, N. A Transwell invasion assay was used to examine the impact of STK39 on MB-231 cell invasion. O, P. Western blot analysis was conducted to evaluate the effects of STK39 on the expression of EMT-related genes. Q-U. Tumor-bearing experiments in nude mice demonstrated that inhibition of STK39 expression significantly reduced tumor proliferation and liver metastasis. ** $P < 0.01$. N-Group: Normal control group; L-group: Lentiviral control group; STK39sh: STK39 gene interference group.

STK39/MAPK14 in triple-negative breast cancer



STK39/MAPK14 in triple-negative breast cancer

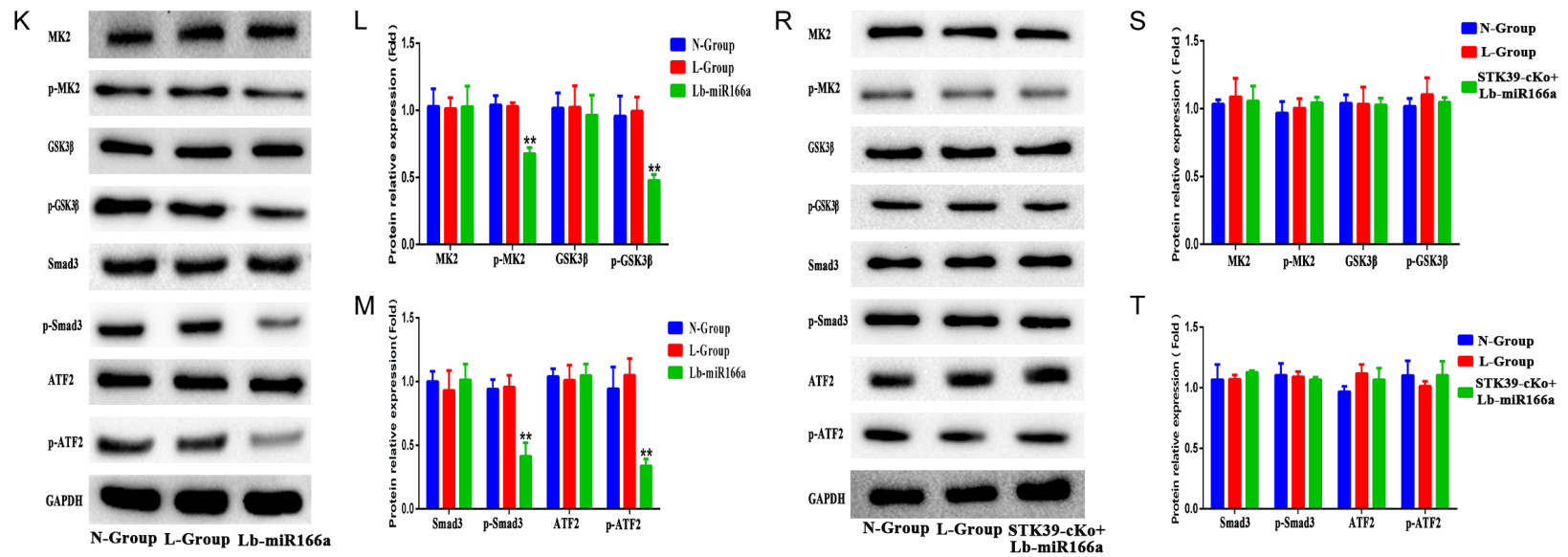


Figure 5. Lb-miR166a modulates the STK39/MAPK14 pathway and inhibits gene phosphorylation. A, B. Demonstration of the STK39 target sequence knockout used in this study. C-F. PCR, western blot, and immunohistochemical analyses indicated no significant differences in STK39 mRNA and protein expression between the N-Group and STK39cKo Group. G-J, N-Q. The expression of STK39 and MAPK14 genes was confirmed by immunofluorescence, RT-PCR, and western blot. K-M, R-T. Western blot was used to measure the protein expression and phosphorylation levels of downstream target genes of MAPK14. **P < 0.01. N-Group: Normal control group; L-group: Lentiviral control group; Lb-miR166a: Lb-miR166a overexpression group; STK39cKo+Lb-miR166a: STK39 target sequence knockout + Lb-miR166a overexpression group.

STK39/MAPK14 in triple-negative breast cancer

cer [15, 17, 18]. However, the molecular mechanisms through which STK39 activates its pro-tumorigenic effects remain largely undefined. Our findings indicate that downregulating STK39 in MB-231 cells significantly inhibits proliferation and promotes apoptosis. We also demonstrate that Lb-miR166a exerts an anti-tumor effect by the STK39/MAPK14 pathway in MB-231 cells.

STK39 is a Ste20-related kinase enriched in alanine and proline, featuring a short N-terminal proline and alanine repeat (PAPA box), a kinase catalytic domain, and a C-terminal regulatory domain [19]. In mammals, STK39 plays a crucial role in ion homeostasis by regulating the activity of cationic chloride co-transporters [20]. Recent research has highlighted STK39's significant role in malignant tumor development, influencing immune cell infiltration, tumor angiogenesis, and epithelial-mesenchymal transition (EMT) [21, 22]. The MAPK pathway is critical for STK39's control of cellular processes such as proliferation, apoptosis, invasion, and metastasis [23]. STK39 induces phosphorylation of MAPK14 [24], and studies have shown that knocking down STK39 restricts tumor growth and invasion in cells such as those of the kidney by inhibiting p38 and MAPK signaling pathways [25].

In our study, we observed that Lb-miR166a regulates the phosphorylation level of MAPK14 by directly targeting STK39, thereby suppressing proliferation and invasion of triple-negative breast cancer cells through the downregulation of phosphorylated MK2, GSK3 β , ATF2, and SMAD3. Typically, MAPK14 resides in the cytoplasm of quiescent cells in an inactive, non-phosphorylated state. Upon activation, phosphorylated MAPK14 translocates to the nucleus, where it phosphorylates over 100 proteins [26]. Many of these proteins are involved in gene expression and regulation, culminating in specific biological functions. Thus, we demonstrated a pivotal role for phosphorylation of MAPK14 in the pathogenesis of triple-negative breast cancer.

Our study has several limitations. First, while we confirmed the role and value of Lb-miR166a in treating triple-negative breast cancer through cell experiments and *in vivo* experiments with nude mice, its clinical application

and safety require further exploration. Second, although we verified that Lb-miR166a regulates the STK39/MAPK14 pathway, thereby inhibiting the proliferation and invasion of triple-negative breast cancer cells, Lb-miR166a may also interact with other relevant signaling pathways. This possibility necessitates further investigation to enable full understanding of its biology.

We showed that the downregulation of STK39 and the inhibition of MAPK14 phosphorylation by Lb-miR166a effectively suppressed the proliferation, migration, and invasion of triple-negative breast cancer cells. These results suggest a promising therapeutic strategy for the treatment of triple-negative breast cancer, highlighting the use of Lb-miR166a as a target for future cancer therapies.

Acknowledgements

The present study was supported by the Key Research and Development Project in Ningxia Hui Autonomous Region (grant no. 2022BEG-03138) and the Research Projects of Ningxia Health and Family Planning Commission (grant no. 2021-NW-007).

Disclosure of conflict of interest

None.

Abbreviations

TNBC, Triple-negative breast cancer; GO, Gene Ontology; KEGG, Kyoto Encyclopedia of Genes and Genomes; Lb-miRNA, Lycium barbarum microRNA; CCK8, Cell counting kit-8; STK39, Serine/threonine-protein kinase 39; MAPK14, Mitogen-activated protein kinase 14; Lb-miR166a, Lycium barbarum miRNA166a; CCND1, cyclin D1; CCNE2, Cyclin E2; CCNA2, Cyclin A2; N-cad, Neuronal cadherin; E-cad, Epithelial cadherin; Cas3, Caspase 3; BCL2, B cell lymphoma 2; BAX, BCL2-associated X protein; MAPK14, mitogen-activated protein kinase 14; EMT, Epithelial-mesenchymal transition; MK2, Mitogen-activated protein kinase-activated protein kinase 2; GSK3 β , Glycogen synthase kinase 3 beta; SMAD3, SMAD family member 3; ATF2, Activating transcription factor 2.

Address correspondence to: Jia Tian, Institute of Medical Sciences, General Hospital of Ningxia Medical University, Key Laboratory of Fertility Preservation and Maintenance of Ministry of Education, Ningxia Medical University, Yinchuan, Ningxia, China. Tel: +86-0951-6880709; E-mail: tianjia042@163.com; Xinlan Liu, Department of Medical Oncology, Ningxia Hui Autonomous Region Hospital, Yinchuan, Ningxia, China. Tel: +86-0951-6744457; E-mail: nxliuxinlan@126.com

References

- [1] Siegel RL, Miller KD and Jemal A. Cancer statistics, 2020. *CA Cancer J Clin* 2020; 70: 7-30.
- [2] Sung H, Ferlay J, Siegel RL, Laversanne M, Soerjomataram I, Jemal A and Bray F. Global cancer statistics 2020: GLOBOCAN estimates of incidence and mortality worldwide for 36 cancers in 185 countries. *CA Cancer J Clin* 2021; 71: 209-249.
- [3] Azamjah N, Soltan-Zadeh Y and Zayeri F. Global trend of breast cancer mortality rate: a 25-year study. *Asian Pac J Cancer Prev* 2019; 20: 2015-2020.
- [4] de Paula B, Kieran R, Koh SSS, Crocama S, Abdelhay E and Muñoz-Espín D. Targeting senescence as a therapeutic opportunity for triple-negative breast cancer. *Mol Cancer Ther* 2023; 22: 583-598.
- [5] Yin L, Duan JJ, Bian XW and Yu SC. Triple-negative breast cancer molecular subtyping and treatment progress. *Breast Cancer Res* 2020; 22: 61.
- [6] Dávalos A, Pinilla L, López de Las Hazas MC, Pinto-Hernández P, Barbé F, Iglesias-Gutiérrez E and de Gonzalo-Calvo D. Dietary microRNAs and cancer: a new therapeutic approach? *Semin Cancer Biol* 2021; 73: 19-29.
- [7] Yang X, Zhang L, Yang Y, Schmid M and Wang Y. miRNA mediated regulation and interaction between plants and pathogens. *Int J Mol Sci* 2021; 22: 2913.
- [8] Lo ACY and Yang M. Lycium barbarum polysaccharides and ferroptosis: jumping into the era of novel regulated cell death. *Neural Regen Res* 2022; 17: 1473-1474.
- [9] Sun L, Zuo C, Liu X, Guo Y, Wang X, Dong Z and Han M. Combined photothermal therapy and lycium barbarum polysaccharide for topical administration to improve the efficacy of doxorubicin in the treatment of breast cancer. *Pharmaceutics* 2022; 14: 2677.
- [10] Zhang Q, Xie Z, Li Y, Zhu Q, Shi H, Zhao R, Yang X, Tian J and Ma L. The potential of Lycium barbarum miR166a in kidney cancer treatment. *Exp Cell Res* 2023; 423: 113455.
- [11] Li C, Wang A, Chen Y, Liu Y, Zhang H and Zhou J. MicroRNA-299-5p inhibits cell metastasis in breast cancer by directly targeting serine/threonine kinase 39. *Oncol Rep* 2020; 43: 1221-1233.
- [12] Rossi L, Longhitano C, Kola F and Del Grande M. State of art and advances on the treatment of bone metastases from breast cancer: a concise review. *Chin Clin Oncol* 2020; 9: 18.
- [13] Samad AFA, Kamaroddin MF and Sajad M. Cross-Kingdom regulation by plant microRNAs provides novel insight into gene regulation. *Adv Nutr* 2021; 12: 197-211.
- [14] Zhang Q, Xie Z, Li Y, Zhu Q, Shi H, Zhao R, Yang X, Tian J and Ma L. Lb-miR166a has a potentially positive impact on the treatment of kidney cancer. 2022; [Epub ahead of print].
- [15] Huang T, Zhou Y, Cao Y, Tao J, Zhou ZH and Hang DH. STK39, overexpressed in osteosarcoma, regulates osteosarcoma cell invasion and proliferation. *Oncol Lett* 2017; 14: 4599-4604.
- [16] Li Z, Zhu W, Xiong L, Yu X, Chen X and Lin Q. Role of high expression levels of STK39 in the growth, migration and invasion of non-small cell type lung cancer cells. *Oncotarget* 2016; 7: 61366-61377.
- [17] Chiu MH, Liu HS, Wu YH, Shen MR and Chou CY. SPAK mediates KCC3-enhanced cervical cancer tumorigenesis. *FEBS J* 2014; 281: 2353-2365.
- [18] Zhao Q, Zhu Y, Liu L, Wang H, Jiang S, Hu X and Guo J. STK39 blockage by RNA interference inhibits the proliferation and induces the apoptosis of renal cell carcinoma. *Onco Targets Ther* 2018; 11: 1511-1519.
- [19] Zhang J, Wang Y, Shen Y, He P, Ding J and Chen Y. G9a stimulates CRC growth by inducing p53 Lys373 dimethylation-dependent activation of Plk1. *Theranostics* 2018; 8: 2884-2895.
- [20] McFarlin BE, Chen Y, Priver TS, Ralph DL, Mercado A, Gamba G, Madhur MS and McDonough AA. Coordinate adaptations of skeletal muscle and kidney to maintain extracellular [K(+)] during K(+)-deficient diet. *Am J Physiol Cell Physiol* 2020; 319: C757-C770.
- [21] Zhang C, Wang X, Fang D, Xu P, Mo X, Hu C, Abdelatty A, Wang M, Xu H, Sun Q, Zhou G, She J, Xia J, Hui KM and Xia H. STK39 is a novel kinase contributing to the progression of hepatocellular carcinoma by the PLK1/ERK signaling pathway. *Theranostics* 2021; 11: 2108-2122.
- [22] Li J, Wang X, Yang J, Zhao S, Liu T and Wang L. Identification of hub genes in hepatocellular carcinoma related to progression and prognosis by weighted gene co-expression network analysis. *Med Sci Monit* 2020; 26: e920854.
- [23] Ni FD, Hao SL and Yang WX. Multiple signaling pathways in Sertoli cells: recent findings in

STK39/MAPK14 in triple-negative breast cancer

- spermatogenesis. *Cell Death Dis* 2019; 10: 541.
- [24] Johnston AM, Naselli G, Gonez LJ, Martin RM, Harrison LC and DeAizpurua HJ. SPAK, a STE20/SPS1-related kinase that activates the p38 pathway. *Oncogene* 2000; 19: 4290-4297.
- [25] Schulz GB, Elezkurtaj S, Börding T, Schmidt EM, Elmasry M, Stief CG, Kirchner T, Karl A and Horst D. Therapeutic and prognostic implications of NOTCH and MAPK signaling in bladder cancer. *Cancer Sci* 2021; 112: 1987-1996.
- [26] Han J, Wu J and Silke J. An overview of mammalian p38 mitogen-activated protein kinases, central regulators of cell stress and receptor signaling. *F1000Res* 2020; 9: F1000 Faculty Rev-653.

STK39/MAPK14 in triple-negative breast cancer

Supplementary Table 1. Sequencing and relative quantification of miRNA in *Lycium barbarum*

miRNA	Read count	Organism	Sequence
miR156a	6	<i>Lycium barbarum</i>	ugacagaagagagugagcac
miR156g	2	<i>Lycium barbarum</i>	cgacagaagagagugagcac
miR156j	31	<i>Lycium barbarum</i>	ugacagaagagagagagcac
miR157a	98	<i>Lycium barbarum</i>	uugacagaagauagagagcac
miR160a	323	<i>Lycium barbarum</i>	ugccuggcucccuugauGCCA
miR162a	12905	<i>Lycium barbarum</i>	ucgauaaaccucugcauccag
miR164a	12465	<i>Lycium barbarum</i>	uggagaagcagggcacgugca
miR164c	138	<i>Lycium barbarum</i>	uggagaagcagggcacgugcg
miR164d	305	<i>Lycium barbarum</i>	uggagaagcagggcacgugcu
miR166a	339307	<i>Lycium barbarum</i>	ucggaccaggcuucauucCCC
miR166b-5p	15	<i>Lycium barbarum</i>	ggaauguugucuggcucgggg
miR166d-5p	753	<i>Lycium barbarum</i>	ggaauguugucuggcucgagg
miR166e-3p	259	<i>Lycium barbarum</i>	ucgaaccaggcuucauucCCC
miR166g-3p	27253	<i>Lycium barbarum</i>	ucggaccaggcuucauucCUC
miR166m	11626	<i>Lycium barbarum</i>	ucggaccaggcuucauucCCU
miR167a	112576	<i>Lycium barbarum</i>	ugaagcugccagcaugaucua
miR167d	3731	<i>Lycium barbarum</i>	ugaagcugccagcaugaucugg
miR167d-5p	3731	<i>Lycium barbarum</i>	ugaagcugccagcaugaucug
miR168a	1808	<i>Lycium barbarum</i>	ucgcuuggugcagggucgggac
miR169h	159	<i>Lycium barbarum</i>	uagccaaggauagacuugccug
miR169t	552	<i>Lycium barbarum</i>	uagccaaggauagacuugccuu
miR171a	6	<i>Lycium barbarum</i>	ugauugagccgcgccaauauc
miR1863a	111	<i>Lycium barbarum</i>	agcucugauaccauguuaguuag
miR211	59542	<i>Lycium barbarum</i>	uaaucugcauccugagguuua
miR2911	85982	<i>Lycium barbarum</i>	ggccgggggacggacuaggga
miR398b	681	<i>Lycium barbarum</i>	uguguucucaggucccccug
miR403	3	<i>Lycium barbarum</i>	uuagauucacgcacaaacucg
miR482c	5898	<i>Lycium barbarum</i>	uuuccuauuccaccaugccaa
miR5072	66	<i>Lycium barbarum</i>	cgauuccccagggagucgcca
miR5538	11	<i>Lycium barbarum</i>	acugaacucaaucacuugcugc
miR6022	2	<i>Lycium barbarum</i>	uggaaggaggaaauuccagga
miR6164a	184	<i>Lycium barbarum</i>	ucacauaaauugaaacggagg